UNIVERSITAT POLITÈCNICA DE CATALUNYA BARCELONATECH

Swansea University Prifysgol Abertawe

CENTRALE NANTES

Universität Stuttgart

MSc in Computational Mechanics

Computational Structural Mechanics and Dynamics

Practice 2: Axisymmetric problems and beam elements

Submitted By:
Mario Alberto Méndez Soto
Eugenio Muttio Zavala

Submitted To:
Prof. Narges Dialami

Spring Semester, 2019

Exercise 1 - Circular tank

Figure (1) shows a circular tank made of reinforced concrete. It is used for the storage of water in a water purification plant. The following material properties are given:

- Concrete $\begin{cases} E = 3.0E10N/m^2 \\ \nu = 00.2 \end{cases}$
- Floor $\begin{cases} \text{Ballast coefficient} = 50N/cm^3 \end{cases}$

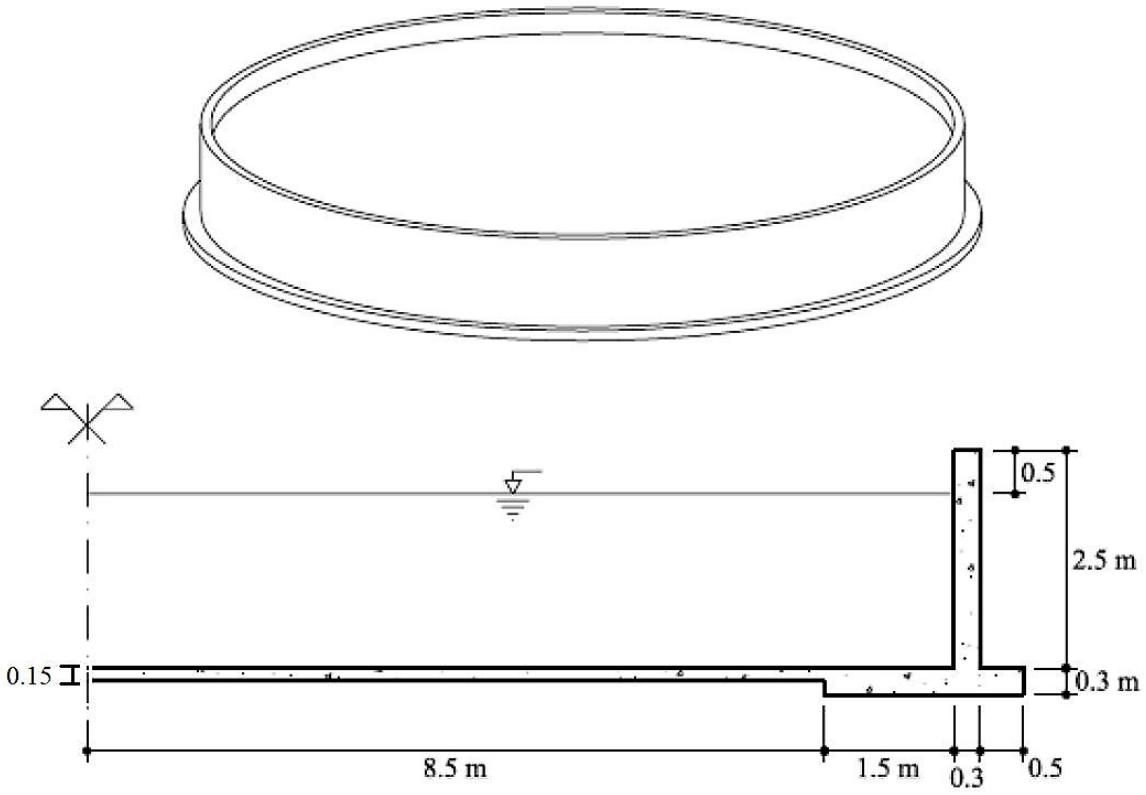

Fig. 1 – Thin plate - geometry and boundary conditions

Given the geometry of the structure, the problem is solved with an axisymmetric formulation using the cross section depicted in Figure (1).

The water column is modeled using two separate hydrostatic distributed loads at the bottom and vertical wall of the tank (maximum value at the bottom equal to $\rho h g_{H_2O} = 24500\ N/m$), whereas, the floor is modeled as an elastic support with a ballast coefficient equal to 50 N/cm^3. The weight of the structure is also taken into account in the computations. Moreover, it is assumed that the ground can only resist compression efforts with no traction or resistance in the x direction allowed. A symmetry condition was imposed on the left boundary of the model, restricting the displacements on the x direction (see Figure (2)).

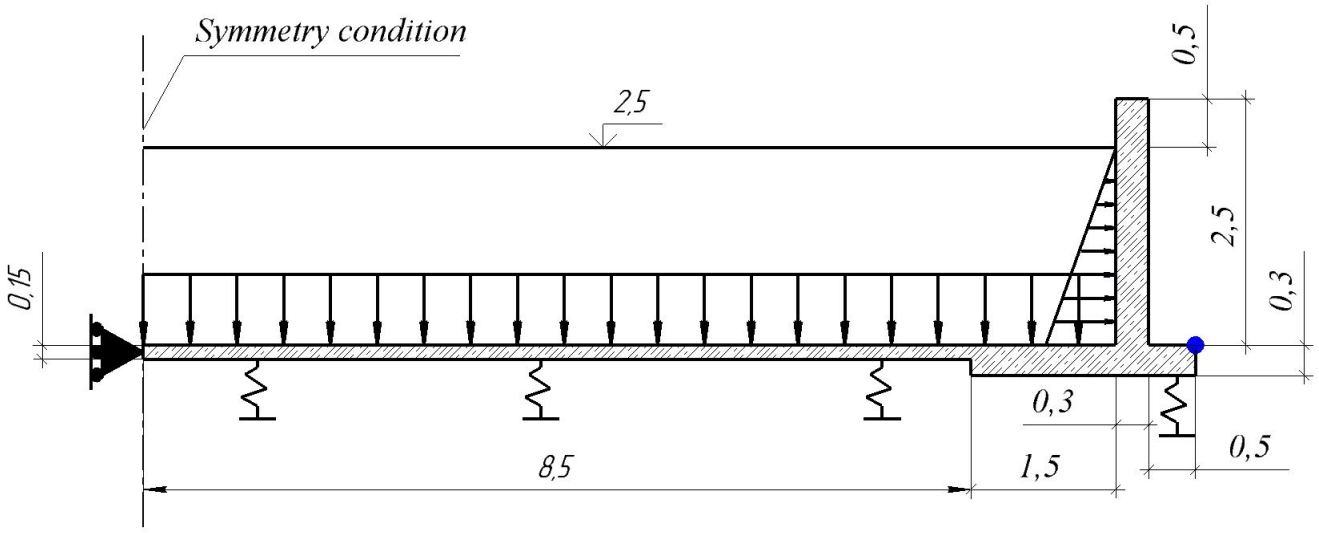

Fig. 2 – Circular tank- geometry and boundary conditions

For the analysis of the problem, the domain was discretized using quadrilateral elements with linear shape functions. A convergence analysis was performed in order to determine the appropriate discretization to obtain results that are independent of the mesh. Hence, an analysis of the behavior of the displacement of a given node (point marked in blue in Figure (2)). Images of the coarsest and finest meshes are presented in Figure (3).

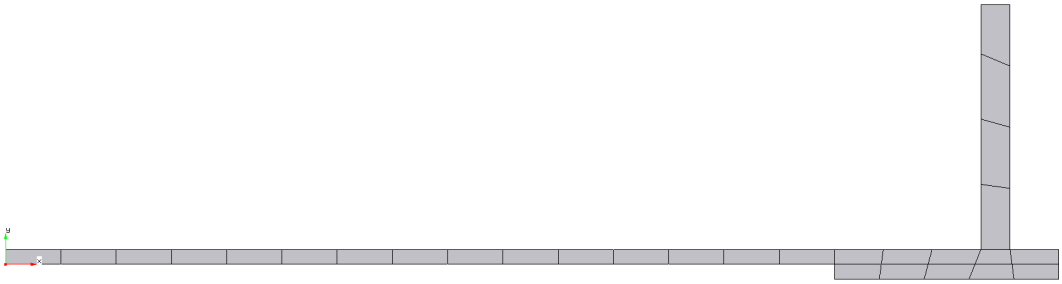

(a) Mesh 1

(b) Mesh 7

Fig. 3 – Sample of meshes used in the convergence study

The results of the convergence analysis are presented in Table (1) and Figure (4). Based on the convergence study, Mesh 6 was chosen.

	Nodes	**Displacement** u_x	**Displacement** u_y
Mesh 1	56	0.0000291519	-0.0002870002
Mesh 2	129	0.0000284567	-0.0002680489
Mesh 3	394	0.0000280268	-0.0002594461
Mesh 4	1143	0.0000278045	-0.0002562074
Mesh 6	3624	0.0000276820	-0.0002548566
Mesh 7	14462	0.0000276193	-0.0002542407

Table 1 – Numerical results of convergence study

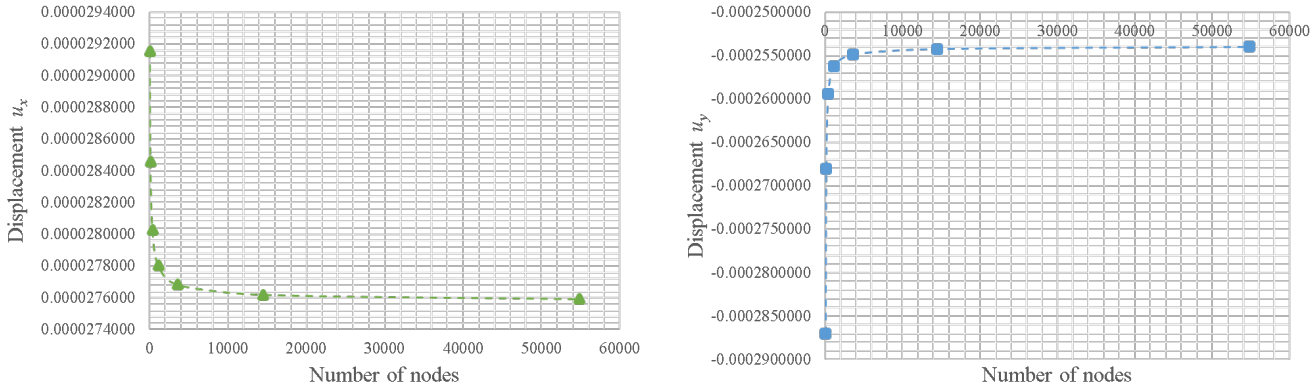

(a) Convergence of displacement u_x

(b) Convergence of displacement u_y

Fig. 4 – Results of convergence study

An analysis of the stress vectors allows us to verify the correctness of the solution, since, as stated before, the floor cannot sustain tension efforts which is satisfied based on the results depicted in Figure (5). Only compression stresses are obtained at the boundary of the floor matching thus the physics of the problem.

The displacements (m) and the corresponding deformed configuration (with a factor of 250) are depicted in Figure (6). The displacements, both in x and y, reach their maximum value at the top of the structure.

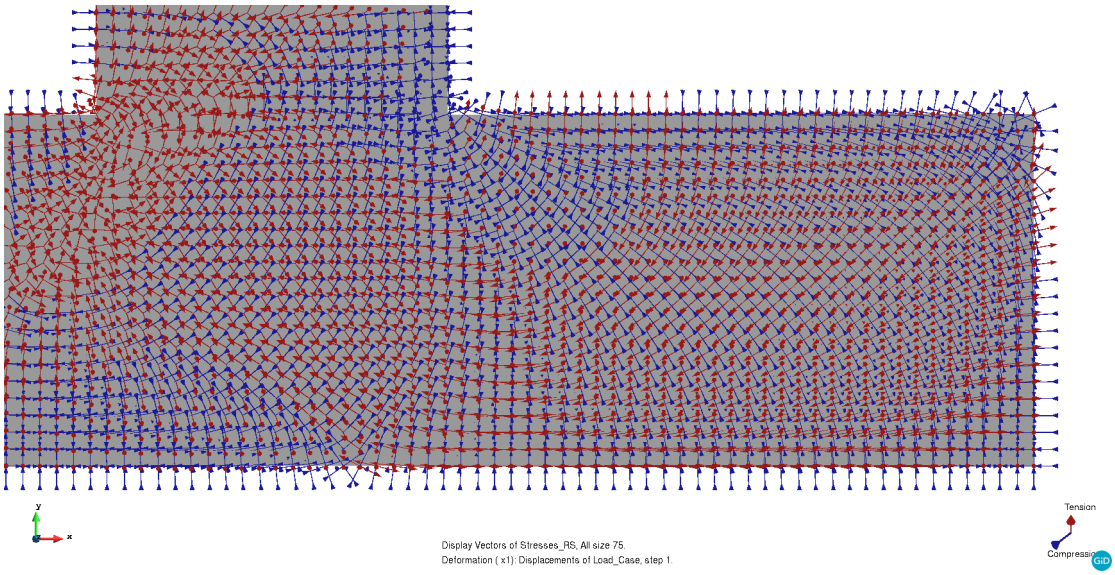

Fig. 5 – Stress vector field at the floor

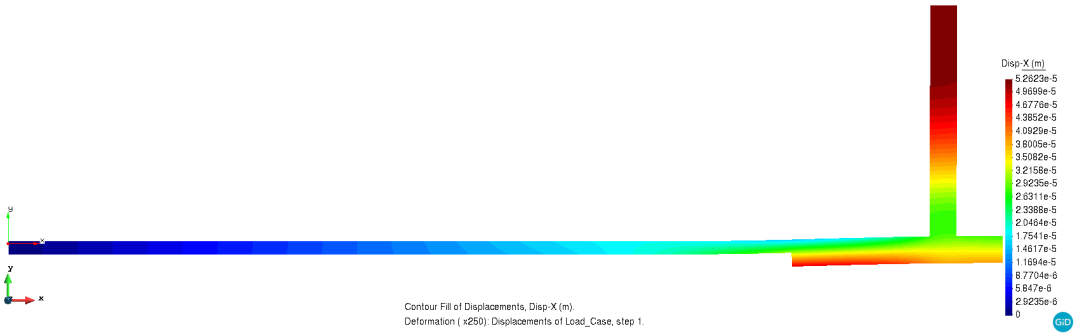

(a) Vector field of displacements u_x

(b) Vector field of displacements u_y

Fig. 6 – Results of displacement vector fields

Exercise 2 - Analysis of the flexion of a beam using hexahedra elements

An reasonable understanding of the capabilities of different types of elements can be achieved by analyzing a problem, whose analytical solution is previously known. Figure (7) shows a 3D cantilever beam, which is by definition a problem characterized as *isostatic* and the solution can be obtained by equilibrium equations. Then a convergence analysis can be implemented in order to verify the exactness of the linear and quadratic hexahedra (8 and 20 nodes respectively).

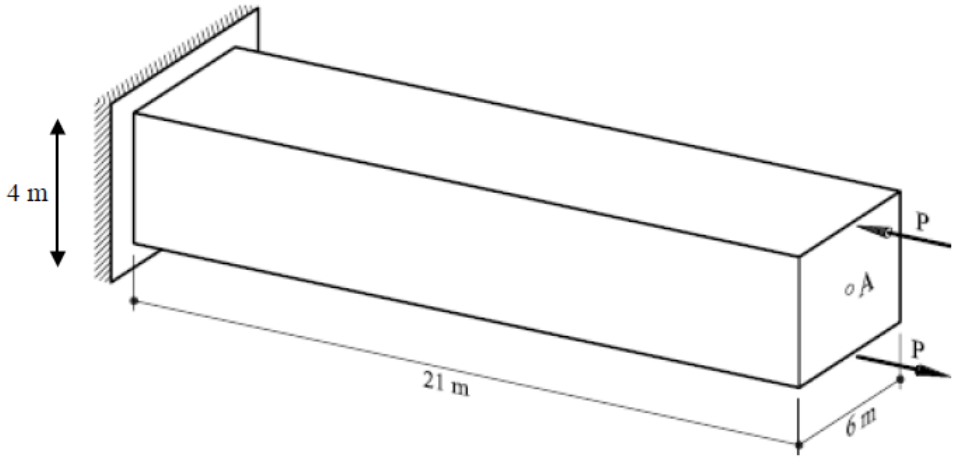

Fig. 7 – Cantiliever Beam.

The problem is modeled in GiD using the FEM solver Ramseries - 3D Elasticity Module. The dimensions, loading and boundary conditions are defined in Figure (7) and the material properties are the following ones:

- Properties $\begin{cases} E = 2.11E11N/m^2 \\ \nu = 0.2 \\ P = 10000N \end{cases}$

The first part of the analysis is to present the analytical procedure using classical beam theory, in which the two forces can be transformed into a moment of magnitude:

$$M = P \cdot l = 10000\ N \cdot \frac{4\ N}{2} = 20000\ Nm \tag{1}$$

Then, the maximum deflection of the beam occurs in point A, whose magnitude is:

$$\delta = \frac{M \cdot L^2}{EI} = \frac{20000\ Nm \cdot (21\ m)^2}{2.11E11N/m^2 \cdot 32\ m^4} = 1.3125E-06\ m \tag{2}$$

In order to obtain a comparison between two degrees of interpolation and the exact solution, several tests varying the discretization of the bar are carried out. Figure (8) shows a comparison of the meshes used.

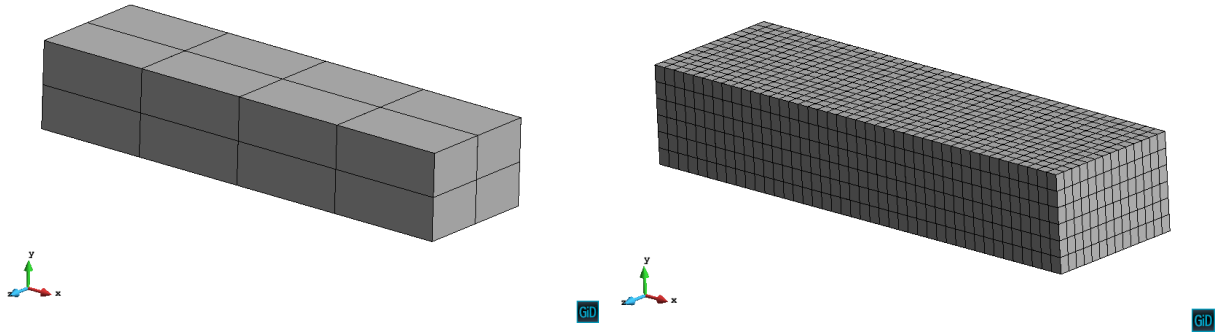

(a) 16 Elements - 45 Nodes (Linear) - 141 (Quad).

(b) 3528 Elements - 4515 Nodes (Linear) - 17009 (Quad).

Fig. 8 – Model discretization, a) coarse mesh and b) fine mesh.

After the FEM solution is found, a comparison of the approximated displacement field can be done (see Figures (9) and (10)).

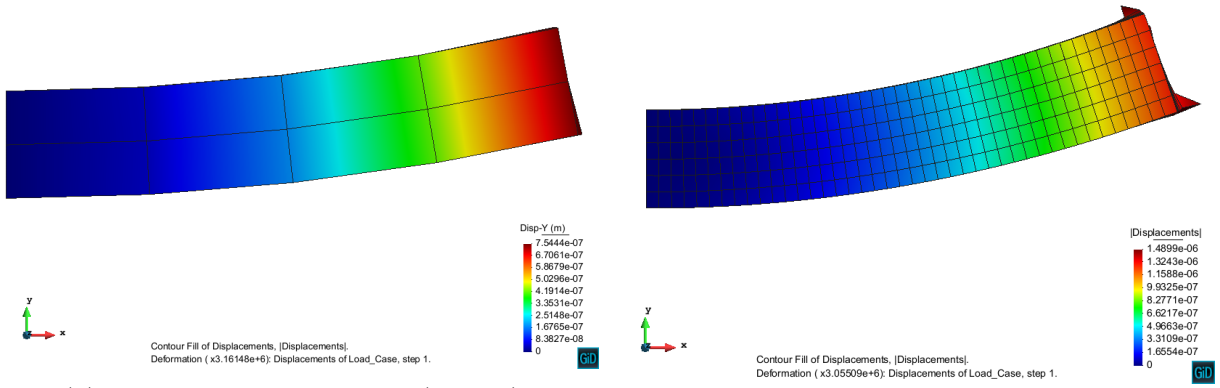

(a) 16 Elements - 45 Nodes (Linear).

(b) 3528 Elements - 4515 Nodes (Linear).

Fig. 9 – Displacement field, a) linear coarse mesh and b)linear fine mesh.

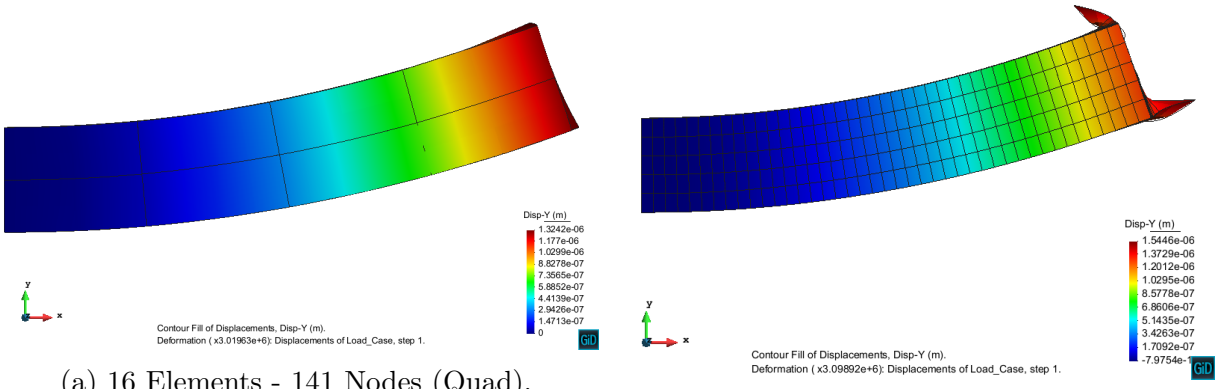

(a) 16 Elements - 141 Nodes (Quad).

(b) 3528 Elements - 17009 Nodes (Quad).

Fig. 10 – Displacement field, a) quadratic coarse mesh and b) quadratic fine mesh.

Subsequently, Figure (11) provides insights into the mathematical trend of the three different cases analysed.

- Analytic Solution
- 8 Node - Hexahedron
- 21 Node - Hexahedron

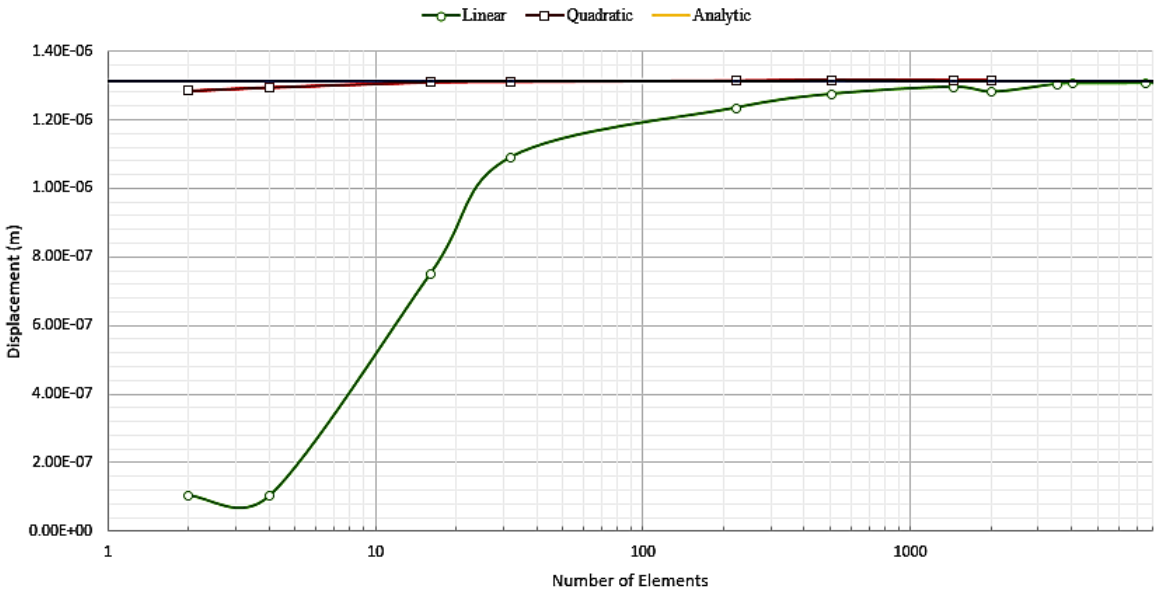

Fig. 11 – Cantiliever Beam Displacement Convergence Graph.

Thus, the results prove that the linear hexadron element provides a quick exponential convergence with reliable results for 200 elements or more. On the other hand, the quadratic element is almost as exact as the analytical approach using as few as 30 elements. The same exactitude can be achieved by the linear element with a 800-element mesh. Hence, a very simplified model can give us a clue about the convergence rate of linear and quadratic elements which can be extrapolate for more complex problems, where the analytical solution is not available. Nevertheless, it is worth mentioning, that although the convergence rate of the quadratic element is better than the linear one, the user should consider its inherent computational cost for more complex problems to be analyzed.

Exercise 3 - Foundation of a corner column.

Figure (12) shows a corner column and its ground foundation. This type of foundation has support reactions that are eccentric with respect to the load of the column resulting in flexion of the column and lifting of the base slab, which is supported elastically by the ground. The mechanical properties of the structure and the soil are indicated below.

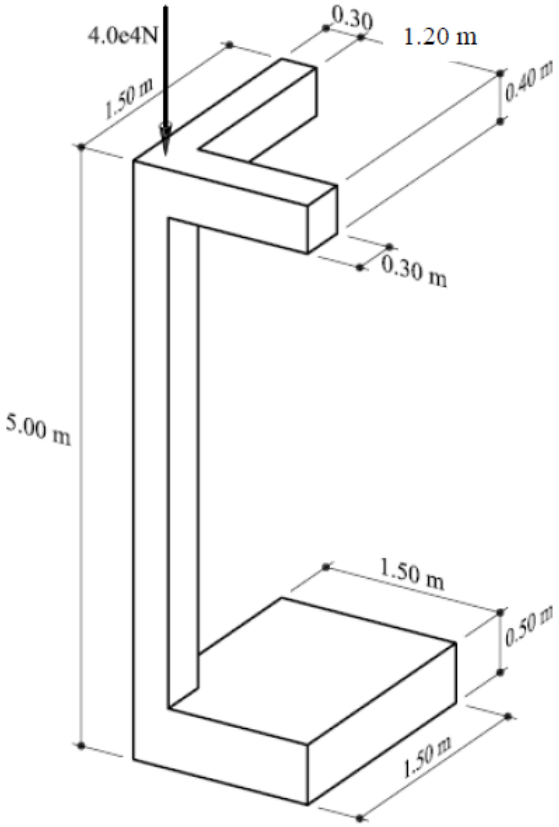

Fig. 12 – Foundation of a corner column.

- Concrete $\begin{cases} E = 3.0E10N/m^2 \\ \nu = 0.2 \\ \gamma = 25000N/m^3 \end{cases}$
- Ground $\begin{cases} \text{Ballast coefficient} = 50N/cm^3 \end{cases}$

The stress state analysis of the foundation is carried out with FEM methodology using Ram-Series solver and the graphical interface GiD. Due to the geometric features of the domain, the computational model was constructed in 3D and discretized with a structured mesh of hexahedrons (eight nodes). A finer mesh was used at the base slab since it requires special treatment that will be discussed further in this work. The discretized domain is shown in Figure 13a.

In light of the fact that the model is a corner foundation of a full structure, symmetry conditions on the beams' cross sections were imposed (motion is constrained in the direction normal to the cross sections). Moreover, the base slab is not completely constrained, instead it is elastically supported the ground. Furthermore, the point load showed in Figure (12) is transformed into an uniform load over the cross section of the column, which is now $4.44E+05N/m^2$. For the analysis, it is considered that the foundation has a volume of ground over the base as it is depicted in Figure (13b).

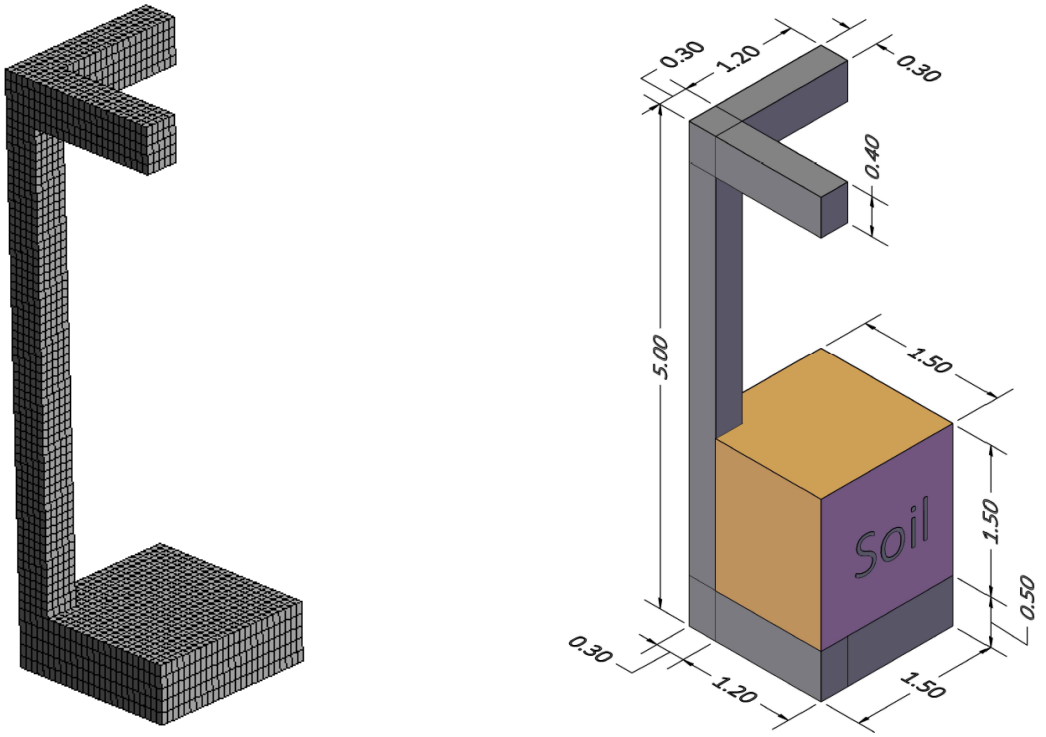

(a) Discretization with 4,850 elements

(b) Ground load considered on the base slab.

Fig. 13 – Discretization and geometric characteristics of the computational domain

After computing the results, a first analysis will be the stress state of the foundation. Figures (14), (15) show that the critical spots (σ_x and σ_y) are around the beams and the connection of the column with the slab. Moreover, Figure (16) shows the stress σ_z in the column due to its deflection. The analysis of σ_x and σ_y is analogous due to the symmetry of the structure, thus it is noticeable in both cases that the maximum value reached is around $8.2E+05$ in compression above the beam and near the uniform load, and $1.2E+06$ in tension under the beam and near the column. As expected, in the slab there is a critical stress value around the connection of the column.

Figure 16 shows the stress field σ_z in the column. As it can be seen, maximum stress value is $1.8E+06$ in compression, and around $4.6E+06$ in tension. Hence, in all cases tension stresses are greater and this should be considered in the concrete reinforcement design.

Important remarks can be made by observing Figure (17), in which shear stresses are depicted. It can be noticed that the greatest shear stresses are located near the column-beam-slab connections.

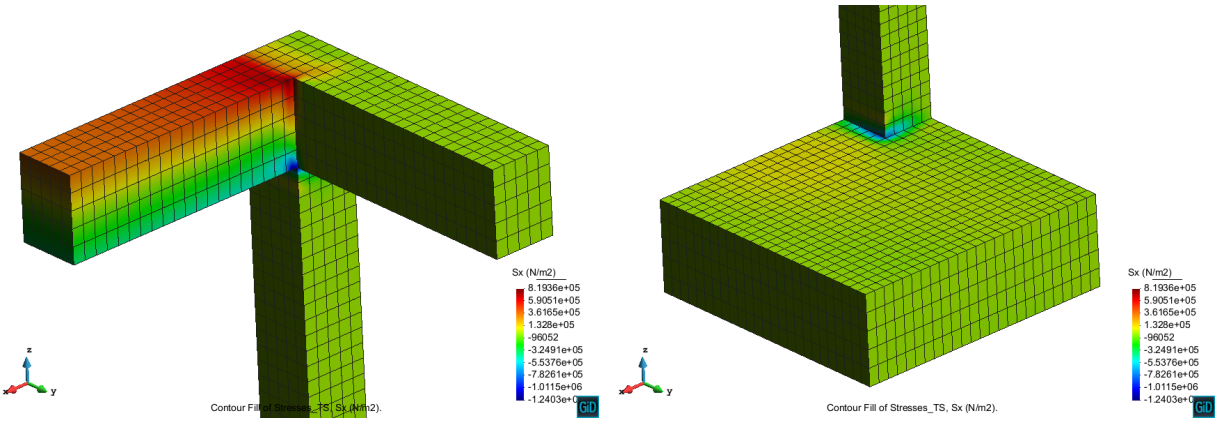

(a) Beams. (b) Base slab.

Fig. 14 – Analysis of σ_x stress in the beams and base slab.

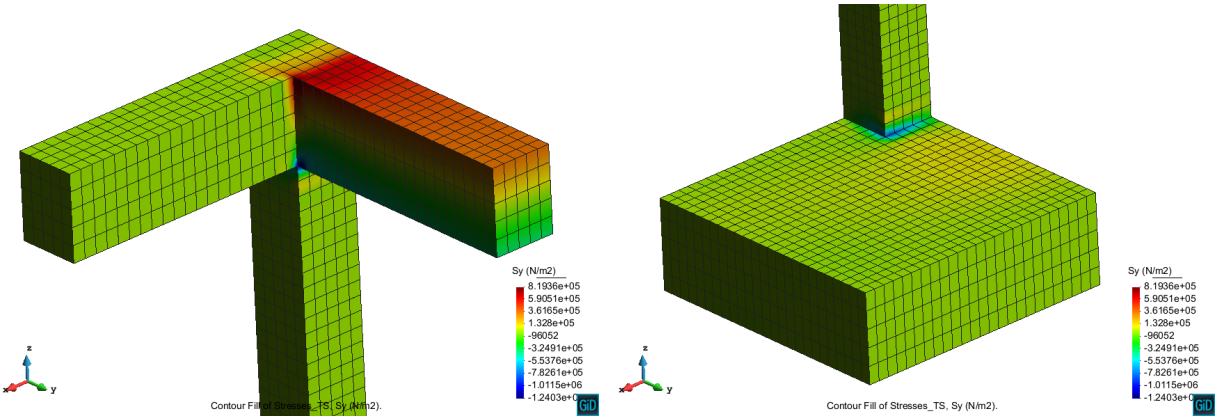

(a) Beams. (b) Base slab.

Fig. 15 – Analysis of σ_y stress in the beams and base slab.

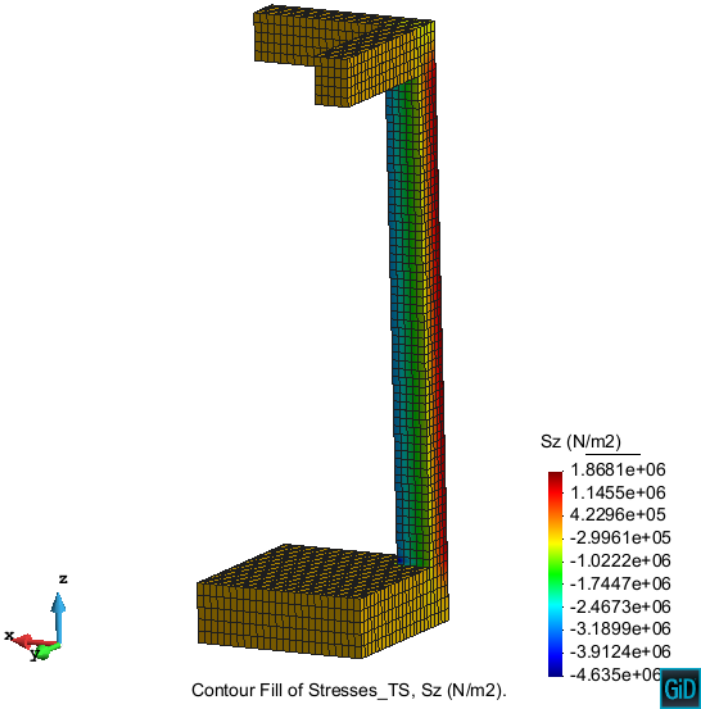

Fig. 16 – Analysis of σ_z stress in the column of the foundation.

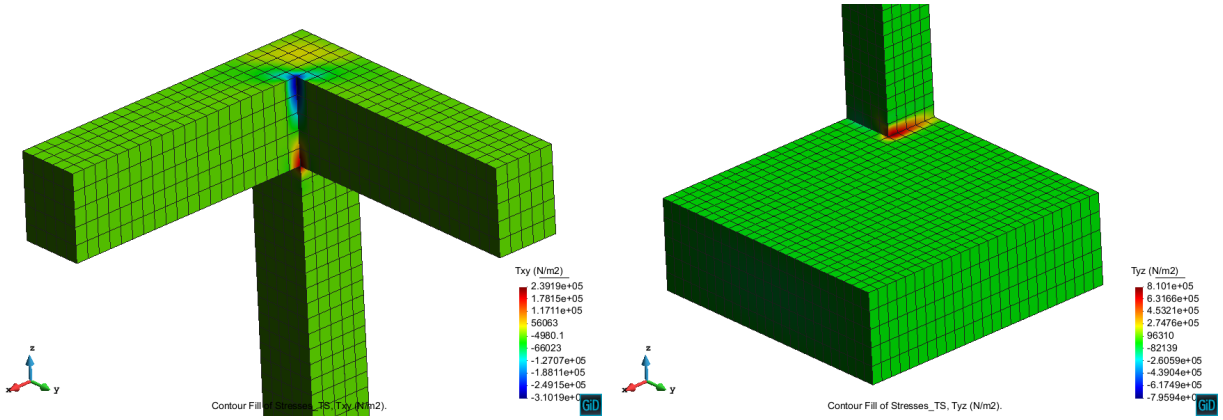

(a) Beams. (b) Base slab.

Fig. 17 – Analysis of τ_{xy} stress in the beam-column connection and τ_{yz} in the column-slab connection.

The principal stresses fields are a representation of the system behavior due the compression and tension effects (Figure 18). The figure shows how force travels in the fibers where flexion is dominant,i.e. column interior and the beams inferior surface. This mechanical effect should be considered carefully in order to design these elements.

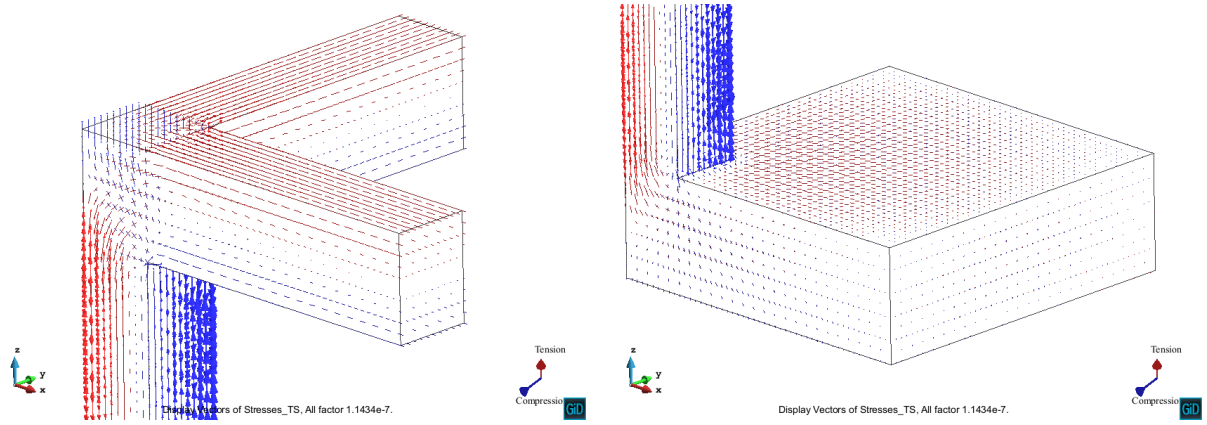

(a) Beams. (b) Base slab.

Fig. 18 – Tension-compression vectors of the principal stresses.

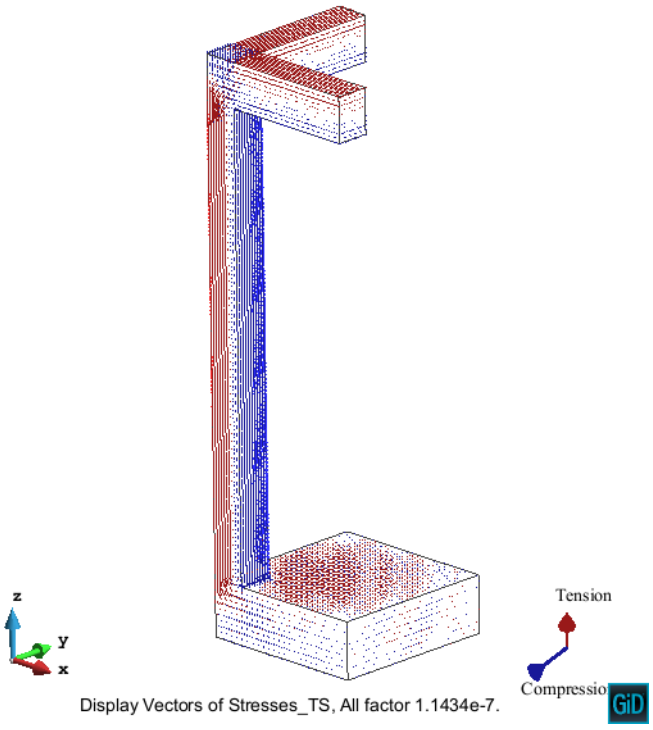

Fig. 19 – Tension-Compression vectors of the principal stresses in the complete system.

Finally the deformed structure is shown in Figure (20). The figure presents the norm of the

displacements in all directions that affects the structure. Special interest should be taken for the *Z-Displacement* in the base slab that shows how **the opposite corner of the column (in the slab) is clearly being lifted off the ground**. This behavior is important to verify because as the soil can not handle tension forces, the design has to consider the lack of traction under the slab.

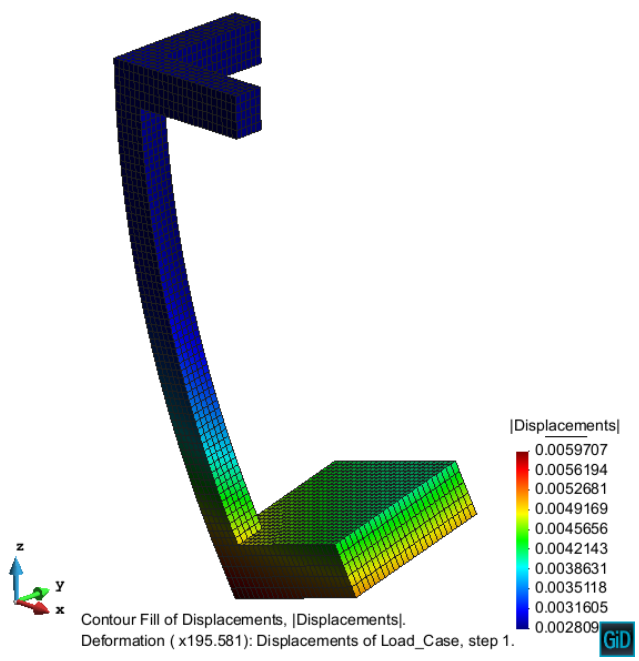

(a) Deformed structure.

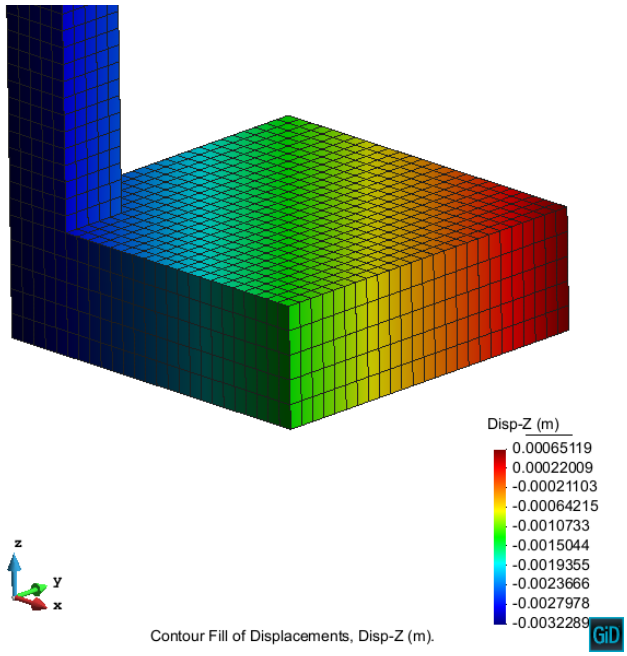

(b) Base slab Z-Deformation.

Fig. 20 – Deformed state and displacement on the base